

Supporting Information

Construction of hierarchical $\text{ZnCo}_2\text{O}_4@(\text{Ni}_x\text{Co}_{2-x})_2(\text{OH})_6$ core/shell nanowire arrays for high-performance supercapacitors

Wenbin Fu,^a Yaling Wang,^a Weihua Han,^{a,*} Zemin Zhang,^a Heming Zha,^b and Erqing Xie^{a,*}

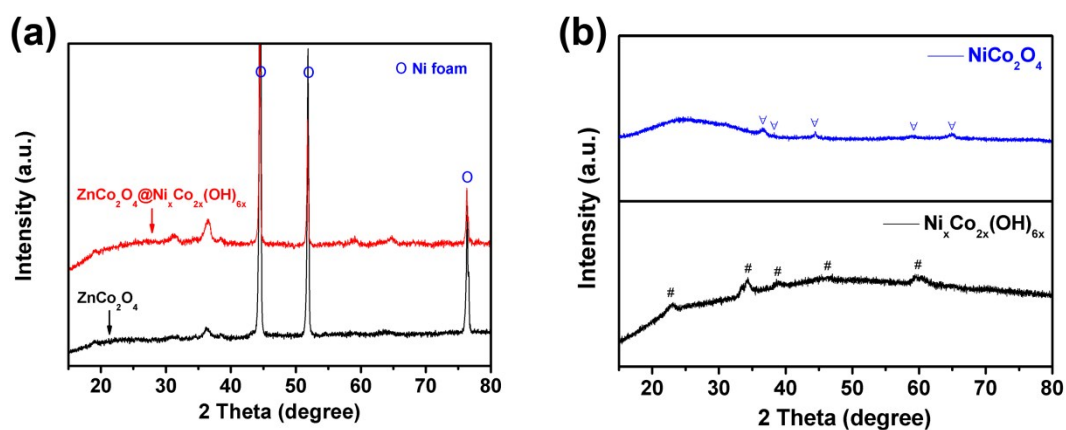


Fig. S1 (a) XRD patterns of the ZnCo_2O_4 NWAs and $\text{ZnCo}_2\text{O}_4@(\text{Ni}_x\text{Co}_{2-x})_2(\text{OH})_6$ NWAs on Ni foam. (b) XRD patterns of $\text{Ni}_x\text{Co}_{2-x}(\text{OH})_6$ nanosheets and converted NiCo_2O_4 after annealing the $\text{Ni}_x\text{Co}_{2-x}(\text{OH})_6$ nanosheets at 400 °C for 2h.

^a School of Physical Science and Technology, Lanzhou University, Lanzhou 730000, China

^b Cuiying Honors College, Lanzhou University, Lanzhou 730000, China.

E-mail: hanwh@lzu.edu.cn (Weihua Han); xieeq@lzu.edu.cn (Erqing Xie). Tel.: +86 931 8912616; Fax: +86 931 8913554.

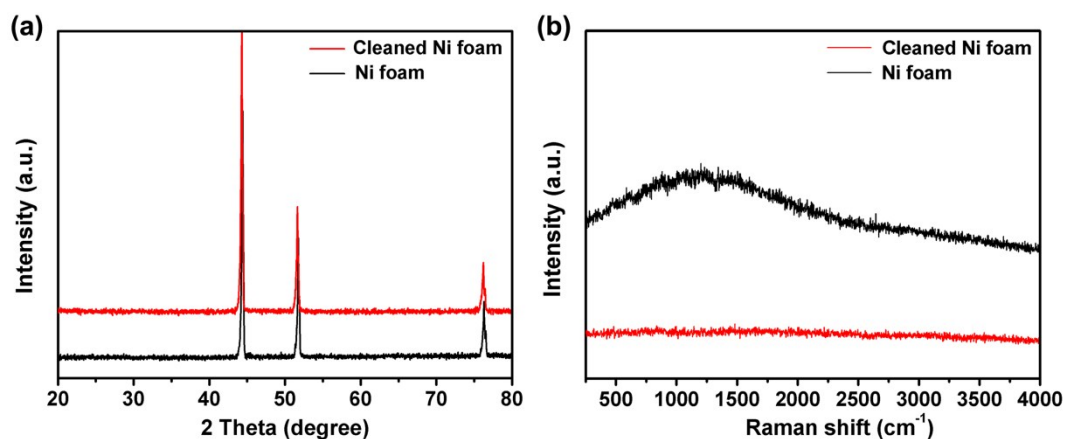


Fig. S2 XRD patterns (a) and Raman spectra (b) of the Ni foam before HCl treatment and the cleaned Ni foam after the treatment.

The Ni foam before HCl treatment and the cleaned Ni foam after this treatment were characterized by XRD and Raman spectroscopy (JY-HR800 micro-Raman, using a 532 nm wavelength YAG laser with a laser spot diameter of about 600 nm). The results are shown in Fig. S2. The strong peaks in the XRD patterns clearly demonstrate the existence of metal Ni and there are no other obvious peaks for additional phases. This could be attributed to the trace mass loading of the oxide layer and impurities. Raman spectra further reveal that most of the oxide layer and impurities have been removed after the treatment.

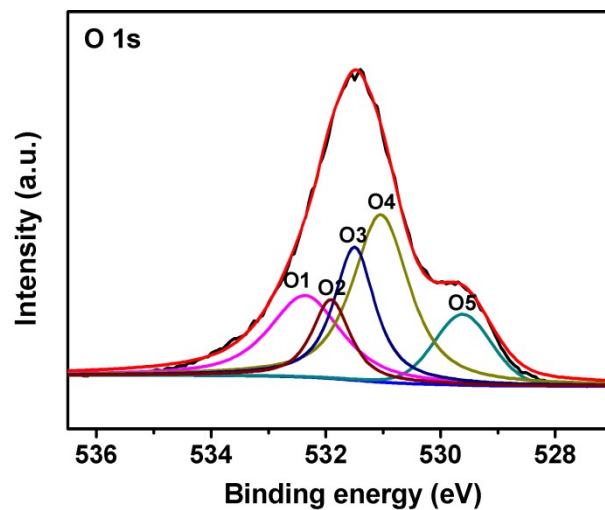


Fig. S3 High-resolution XPS spectra of O 1s for ZnCo₂O₄@Ni_xCo_{2-x}(OH)₆.

Fig. S3 shows that the O 1s spectra is complex and can be fitted with five peaks (O1, O2, O3, O4 and O5). The O3 peak at 531.5 eV and O5 peak at 529.6 eV can corresponded to the oxygen species in ZnCo₂O₄ (Ref. 47). The O2 peak at 531.9 eV and O5 peak at 531 eV should be assigned to the Ni-O-H and Co-O-H bands in Ni_xCo_{2-x}(OH)₆. The O1 peak can be attributed to physisorbed and chemisorbed water. (Ref. 20)

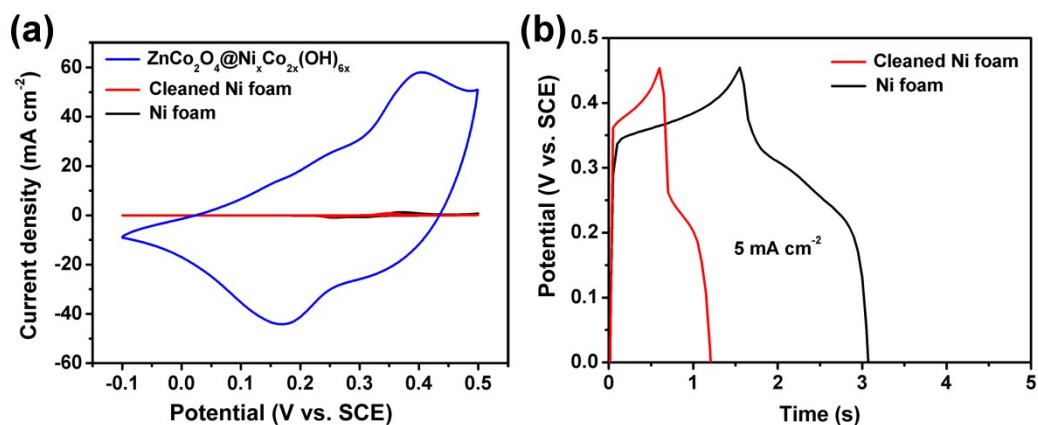


Fig. S4 (a) A comparison of CV curves for the Ni foam, cleaned Ni foam and $\text{ZnCo}_2\text{O}_4@\text{Ni}_x\text{Co}_{2x}(\text{OH})_{6x}$ electrode at the scan rate of 10 mV s^{-1} . (b) GCD curves of Ni foam and cleaned Ni foam at the current density of 5 mA cm^{-2} .

As shown in Fig. S4a, the integrated area for the Ni foam and cleaned Ni foam is very negligible when compared with that of the $\text{ZnCo}_2\text{O}_4@\text{Ni}_x\text{Co}_{2x}(\text{OH})_{6x}$ electrode, suggesting the capacity contribution from the Ni foam and cleaned Ni foam can be neglected. GCD curves further confirmed their limited capacity. The calculated areal capacity for the Ni foam is about $2.09 \mu\text{Ah cm}^{-2}$ ($\sim 0.5\%$ of that of the $\text{ZnCo}_2\text{O}_4@\text{Ni}_x\text{Co}_{2x}(\text{OH})_{6x}$ electrode) while the areal capacity for the cleaned Ni foam is only $0.84 \mu\text{Ah cm}^{-2}$ ($\sim 0.2\%$ of the value of the $\text{ZnCo}_2\text{O}_4@\text{Ni}_x\text{Co}_{2x}(\text{OH})_{6x}$ electrode) at a current density of 5 mA cm^{-2} . It is well noted that the contributed capacity for both the Ni foam and HCl cleaned Ni foam can be neglected. In our study, we ultrasonically cleaned the Ni foam with acetone, 3 M HCl solution, deionized water and ethanol for 15 min each to remove the impurities and oxide layer. This treatment can make our results more accurate and meaningful.

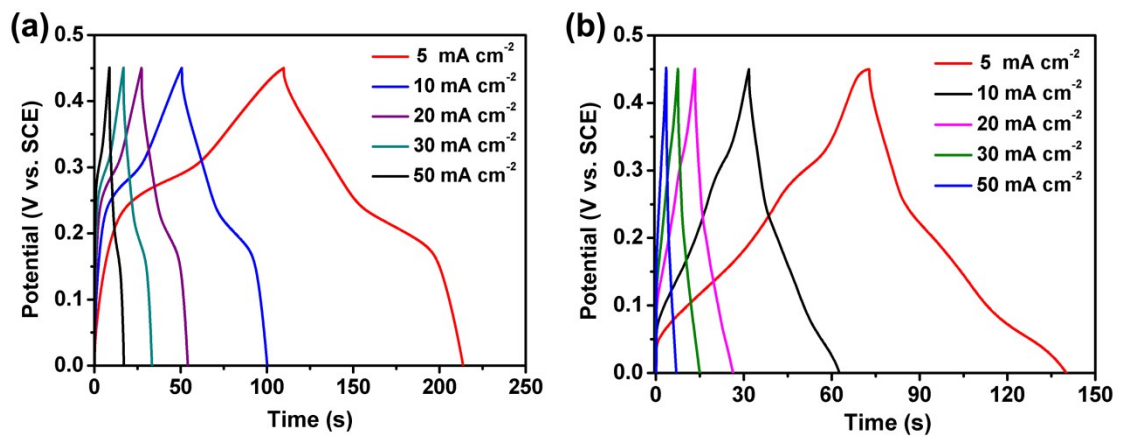


Fig. S5 GCD curves of as-prepared ZnCo₂O₄ (a) and Ni_xCo_{2x}(OH)_{6x} (b) electrodes.

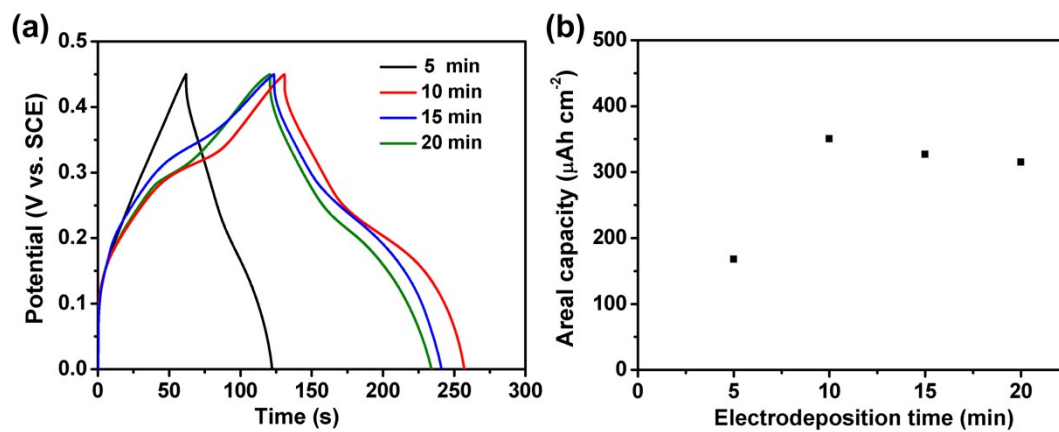


Fig. S6 GCD curves (a) and areal capacity (b) of the ZnCo₂O₄@Ni_xCo_{2x}(OH)_{6x} electrodes with various deposition time of Ni_xCo_{2x}(OH)_{6x} nanosheets.

Table S1 The obtained values of R_s , R_{ct} and W for the $ZnCo_2O_4$, $Ni_xCo_{2-x}(OH)_{6x}$ and $ZnCo_2O_4@Ni_xCo_{2-x}(OH)_{6x}$ electrodes.

Electrode	R_s	R_{ct}	W
$ZnCo_2O_4$	0.96	0.68	0.14
$Ni_xCo_{2-x}(OH)_{6x}$	0.82	2.02	0.22
$ZnCo_2O_4@Ni_xCo_{2-x}(OH)_{6x}$	0.75	1.12	0.18

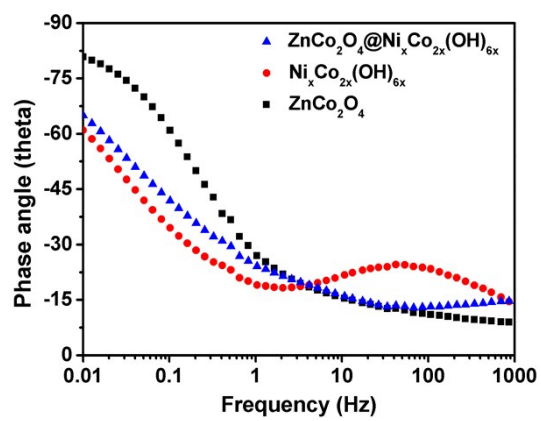


Fig. S7 Bode plots of the $\text{ZnCo}_2\text{O}_4@ \text{Ni}_x\text{Co}_{2x}(\text{OH})_{6x}$, $\text{Ni}_x\text{Co}_{2x}(\text{OH})_{6x}$ and ZnCo_2O_4 electrodes.

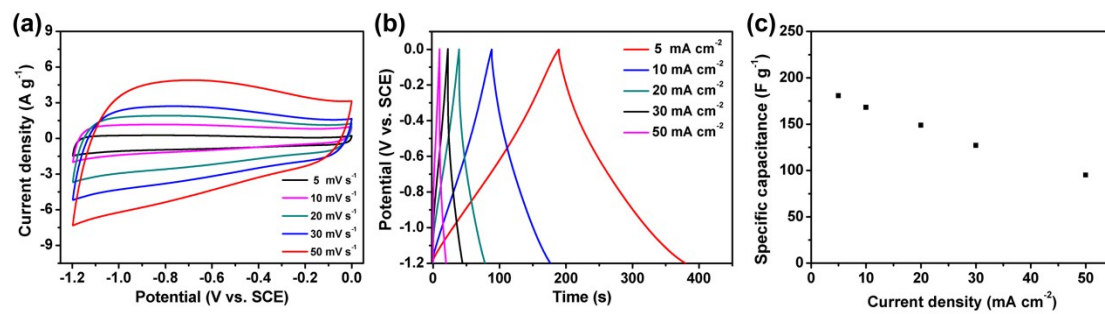


Fig. S8 CV curves (a) and GCD curves (b) of AC. (c) Specific capacitance of AC at different current densities.

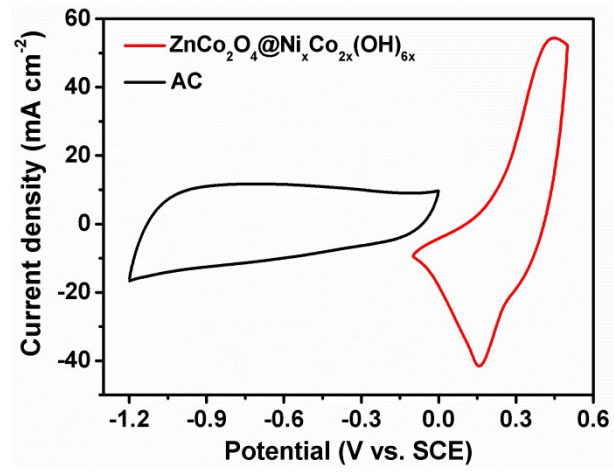


Fig. S9 CV curves of the prepared ZnCo₂O₄@Ni_xCo_{2x}(OH)_{6x} and AC electrodes at 20 mV s⁻¹.

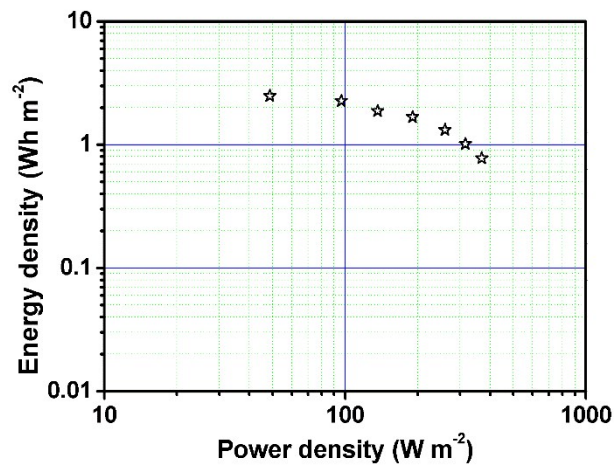


Fig. S10 Areal energy density and power density of the ZnCo₂O₄@Ni_xCo_{2x}(OH)_{6x}//AC hybrid supercapacitor.